The Journal of Experimental Biology 212, 843-852
Published by The Company of Biologists 2009
doi:10.1242/jeb.025999

The effects of thermally induced gill remodeling on ionocyte distribution and branchial chloride fluxes in goldfish (*Carassius auratus*)

D. Mitrovic and S. F. Perry*
Department of Biology, 30 Marie Curie, Ottawa, ON, Canada, K1N 6N5
*Author for correspondence (e-mail: sfperry@uottawa.ca)

Accepted 15 December 2008

SUMMARY

Experiments were performed to evaluate the effects of temperature-induced changes in functional gill lamellar surface area on the distribution of ionocytes and branchial chloride fluxes in goldfish (*Carassius auratus*). In fish acclimated to warm water (25°C), the ionocytes were scattered along the lamellae and within the interlamellar regions of the filament. In cold water (7°C), the ionocytes were largely absent from the lamellae and filaments but instead were mostly confined to the outer regions of an interlamellar cell mass (ILCM) that formed within the interlamellar channels. Using a 'time-differential double fluorescent staining' technique, it was determined that in fish transferred from 25° to 7°C, the ionocytes on the outer edge of (and within) the ILCM originated predominantly from the migration of pre-existing ionocytes and to a lesser extent from the differentiation of progenitor cells. Despite the greater functional lamellar surface area in the warm-water-acclimated fish, there was no associated statistically significant increase in passive branchial Cl^- efflux. Because the paracellular efflux of polyethylene glycol was increased 2.5-fold at the warmer temperature, it would suggest that goldfish specifically regulate (minimize) Cl^- loss that otherwise would accompany the increasing functional lamellar surface area. In contrast to predictions, the numbers and sizes of individual ionocytes was inversely related to functional lamellar surface area resulting in a markedly greater ionocyte surface area in fish acclimated to cold water (5219±438 compared with 2103±180 $\mu m^2 mm^{-1}$ of filament). Paradoxically, the activity of Na^+/K^+-ATPase (as measured at room temperature) also was lower in the cold-water fish (0.43±0.06 compared with 1.28±0.15 $\mu mol\ mg^{-1}$ protein h^{-1}) despite the greater numbers of ionocytes. There were no statistically significant differences in the rates of Cl^- uptake in the two groups of fish despite the differences in ionocyte abundance. It is possible that to maintain normal rates of Cl^- uptake, a greater ionocyte surface area is required in the cold-water fish that possess an ILCM because of the unfavorable positioning of the ionocytes on and within the ILCM, a structure lacking any obvious blood supply.

Key words: gill, mitochondrion rich cell, ionocyte, chloride cell, osmorespiratory compromise, paracellular permeability, ionic regulation, Na^+/K^+-ATPase.

INTRODUCTION

The fish gill (Evans et al., 2005) is the site of numerous physiological processes including chemoreception (Burleson et al., 1992; Burleson, 1995; Jonz et al., 2004; Burleson et al., 2006; Gilmour and Perry, 2007), hormone metabolism (Olson, 1998; Olson, 2002), acid–base regulation (Claiborne, 1998; Perry and Gilmour, 2006), excretion of nitrogenous wastes (Wood, 1993; Wright, 1995) gas exchange (Randall and Daxboeck, 1984; Perry and McDonald, 1993; Gilmour, 1997; Perry and Gilmour, 2002; Nikinmaa, 2006) and ionic regulation (Goss et al., 1992; Evans et al., 1999; Marshall and Grosell, 2006; Hwang and Lee, 2007). Elements of these physiological functions, in particular the diffusive component of gas transfer, require a large functional surface area. In the fish gill, surface area is markedly increased by the presence of thousands of highly vascularized lamellae that project from gill filaments (Laurent and Dunel, 1980; Laurent, 1984; Wilson and Laurent, 2002). The spaces between adjacent lamellae through which ventilatory water flows are termed the interlamellar channels. Functional surface area is labile and typically is adjusted in a regulated fashion according to metabolic requirements or environmental conditions. There are distinct advantages associated with such dynamic adjustments of surface area. Essentially, factors favoring high rates of branchial gas transfer (e.g. high surface area) will also result in higher rates of obligatory salt and water movements across the gill (Randall et al., 1972; Gonzalez and McDonald, 1992). Because of the relatively high costs of actively absorbing salts in freshwater (FW) and actively excreting salts in seawater, functional surface area may be dynamically modified to match gas transfer requirements; a phenomenon termed the osmorespiratory compromise. Thus, by maintaining surface area as low as is possible, the obligatory movements of salt and water across the gill are reduced and hence the energetic costs of ion pumping are minimized. Acute changes in functional surface area can be achieved by recruiting previously unperfused lamellae (lamellar recruitment) or by more uniformly perfusing individual lamellae (Booth, 1979; Farrell et al., 1980). Chronic (hours to days) and occasionally extreme changes in functional surface area are accomplished in some species by physical covering/uncovering of lamellae (Sollid et al., 2003; Metz et al., 2003; Brauner et al., 2004; Sollid et al., 2005; Ong et al., 2007) (for reviews, see Sollid and Nilsson, 2006; Nilsson, 2007). Crucian carp (*Carassius carassius*), common carp (*Cyprinus carpio*) goldfish (*Carassius auratus*) and mangrove killifish (*Kryptolebias marmoratus*) exhibit reversible gill remodeling in accordance with changes in O_2 demand or availability, whereas *Arapaima gigas* exhibits a permanent remodeling of lamellar structure in association with a developmental transition from water- to air-breathing (Brauner et al., 2004). Though the signaling mechanisms are unknown, gill remodeling is accomplished by the invasion or

retraction of an interlamellar cell mass (ILCM) by cell proliferation and apoptosis, respectively (Sollid et al., 2003).

In goldfish, the ILCM is present in fish acclimated to cold normoxic water, but is retracted in fish exposed to waters of increasing temperature (Sollid et al., 2005). Thus, in the present study, acclimation to two different temperatures (7° and 25°C) was used as a tool to cause gill remodeling and elicit two distinct phenotypes. The fish acclimated to 7°C would have an ILCM and hence reduced functional lamellar surface area whereas the fish acclimated to 25°C would have little or no ILCM and hence increased functional lamellar surface area.

These differing branchial phenotypes at the different ambient temperatures are expected to significantly impact ionic regulation because of differences in functional lamellar surface areas and the consequences of the presence or absence of an ILCM on the distribution of ion transporting cells (see below). In the present study we have specifically focused on the consequences of gill remodeling on branchial Cl^- fluxes. In FW fish, the mitochondrion rich cell (MRC) or FW chloride cell (Perry, 1997) is believed to be the cell type responsible for Cl^- uptake (Perry, 1997; Perry et al., 2003b; Tresguerres et al., 2006). Because there are numerous subtypes of fish MRC that may transport different ions, use of the term 'ionocyte' is gaining favor to denote generically all members of the MRC family (Hwang and Lee, 2007).

With this background, two hypotheses were formulated. First, because the ionocytes typically located at the base of filaments within the interlamellar regions might become inoperable owing to their covering by the ILCM, it is hypothesized that ionocytes will migrate with the ILCM to remain perpetually exposed to the water so as to maintain the potential for Cl^- uptake. Second, it was reasoned that an increased surface area at higher temperature would increase passive Cl^- loss which would need to be matched by equivalent increases in Cl^- uptake, necessitating an increase in the ion transporting capacity of the gill. Thus, we hypothesize that increased functional lamellar surface area in goldfish acclimated to warm water will increase Cl^- efflux that will be matched by increased Cl^- uptake owing to an increase in the numbers of ionocytes.

MATERIALS AND METHODS

Experimental animals

All experiments were performed according to the University of Ottawa institutional guidelines, which comply with those of the Canadian Council on Animal Care (CCAC). Goldfish, *Carassius auratus* weighing, on average, 23.9±0.4 g, N=207) were obtained from Along's International (Mississauga, Canada). They were first acclimated to 18°C in large fiberglass tanks filled with dechlorinated tap water. After at least 1 week, temperatures were either increased or decreased 2°C per day to achieve final acclimation temperatures of 7° or 25°C. Animals were kept in the facility under a 12 h:12 h light:dark photoperiod and were fed once a day with commercial food pellets. Fish were kept under such conditions for at least 2 weeks prior to their use in experiments. Twenty-four hours prior to any experiment, fish (including controls) were moved from their holding tanks to individual boxes (approximately 600 ml water volume) provided with flowing aerated water at the appropriate acclimation temperature; fish were not fed.

At the end of each experiment, fish were killed by anesthetic overdose using a solution of benzocaine (ethyl-*P*-amino-benzoate, 2.4×10^{-4} mol l^{-1}; Sigma, St Louis, MO, USA) and gill tissue was removed and processed for light microscopy, immunocytochemistry, Na^+/K^+-ATPase (NKA) activity and real-time reverse transcription PCR (real-time RT-PCR). For some experiments, blood and water samples were also collected.

Light microscopy and immunocytochemistry

Upon removal of the gill arches, filaments from arches 1 and 2 (left side) were placed into a solution of zinc iodide–2% osmium tetroxide (3:1 ratio) for at least 24 h at room temperature (Garcia-Romeu and Masoni, 1970). The samples were then cryoprotected using 15% sucrose (12 h) followed by 30% sucrose. All samples were stored in 30% sucrose at 4°C prior to use. The gills were embedded in OCT cryosectioning medium (VWR, Mississauga, ON, Canada), incubated for 20 min and sectioned horizontally (10 μm section) using a cryostat (Leica CM 1850 Laboratories Eq., Nussloch, Germany). Sections were placed on microscopy slides (Superfrost Plus; Fisher, Ottawa, ON, Canada) and mounted with 60% glycerol under a coverslip.

For immunocytochemistry, gill filaments from arches 1 and 2 (right side) were placed directly into 4% paraformaldehyde and left overnight at 4°C. Tissues were cryoprotected in sucrose and sectioned (10 μm thick sections) using a cryostat (see above). Sections were placed on microscopy slides (Superfrost Plus; Fisher) and allowed to incubate for 1 h at room temperature prior to being stored at 4°C until required. Following 3× 5 min washes with PBST (0.1 mol l^{-1} phosphate-buffered saline, 0.3% Triton-X 100) and blocking with sheep serum (1:10 dilution; Sigma) for 1 h, sections were incubated for 2 h at room temperature with primary antibody: α5 (1:100), a mouse monoclonal antibody against the α1 sub-unit of chicken Na^+/K^+-ATPase (University of Iowa Hybridoma Bank). The α5 antibody has been used successfully for immunocytochemistry in numerous vertebrate species including fish (e.g. Wilson et al., 2000). For negative controls, sections were incubated with 1× PBST buffer lacking primary antibody. Immunofluorescence was detected after incubating the sections with a 1:400 dilution of Alexa Fluor 546 coupled to goat anti-mouse IgG (Fisher) for 1 h. After washing (3× 10 min in 0.1× PBS), sections were mounted in Vectashield mounting medium (Vector Labs, Burlingame, MA, USA) and a coverslip placed on top.

For each fish, two gill sections were examined using light or epifluorescence microscopy. Photos (four per fish) from 'randomly' selected areas of the mid regions of the gill filament were taken at 40× magnification. Photos were taken using an Axiophot (Zeiss, Munich, Germany) microscope, Olympus DP70 digital microscope camera and Image Pro Plus software, Version 6.0 (Media Cybernetics, Bethesda, USA). Typically, the photos would span approximately 0.2 mm of filament length over which there would be 9–11 lamellae; a single filament and associated lamellae were analyzed per photo. Digital images were analyzed using web-based imaging software (Image J, Waine Rasband, MD, USA) to determine morphological variables including numbers and two-dimensional surface areas of ionocytes (as identified using zinc iodide-osmium tetroxide staining or NKA immunofluorescence) and the relative surface area of the ILCM.

Na^+/K^+ ATPase activity

The third gill arch from each fish was added to SEI buffer (150 mmol l^{-1} sucrose, 10 mmol l^{-1} EDTA, 50 mmol l^{-1} imidazole), frozen in liquid N_2 and stored at –80°C. Na^+/K^+ ATPase activity, in the supernatant of homogenized samples, was determined at room temperature (in triplicate) using a spectrophotometric microplate assay according to the method of McCormick (McCormick, 1993). Ouabain-sensitive ATPase activity was measured and expressed as μmoles ADP mg^{-1} protein h^{-1} and compared with ATPase activity in the absence of ouabain. Protein was determined using the bichinchonic acid method (Bio-Rad, Hercules, CA, USA) accorder to the instructions of the manufacturer.

Real-time RT-PCR

Total RNA was extracted from 100 mg of gill tissue using TRIzol Reagent (Invitrogen, Carlsbad, CA, USA) and re-suspended in 40 µl of nuclease-free water. Reverse transcription was performed using the Revertaid H Minus M-MuLV reverse transcriptase enzyme according to the protocol for cDNA synthesis provided by the manufacturer (Fermentas, Life Sciences, Burlington, ON, Canada). The following modifications were made: the final reaction volume was 20 µl and 2 µl of RNA was used with 0.2 µg or random hexamer primers. An MX 3000 Multiplex Quantitative PCR System (Stratagene) and Brilliant SYBR Green QPCR Master Mix (Stratagene) were used for the real-time RT-PCR as per the manufacturer's instructions, with slight modifications: the total reaction volume was adjusted to 12.5 µl, 1 µl of cDNA template was used and final primer concentrations were 100 nmol l^{-1}. Annealing and extension temperatures were 55°C (1 min) and 72°C (1 min) for 40 cycles. All the primers used for real-time PCR (including the reference gene 18S ribosomal RNA) were designed using web-based software (primer3; http://frodo.wi.mit.edu/cgi-bin/primer3/primer3_www.cgi). To obtain homologous primers to amplify goldfish NKA, a 485 bp nucleotide sequence obtained from a BLAST search of GenBank (accession no. FG392680) was used: NKA 1α (09a01); forward primer 5′-CGAGGTACCGTCACCATTCT-3′, reverse primer 5′-GTCTGTTTTGGGGTTTCTGG-3′. These primers were designed to yield an amplicon of 123 base pairs. The specificity of the primers was verified by cloning and sequencing of the amplified product. A blastn search of GenBank indicated that the PCR product was most similar to zebrafish ATPase, Na^+/K^+ transporting, alpha 1 polypeptide (atp1a1 also known as atp[a]1B1). This subunit is probably orthologous to the Na^+/K^+-ATPase alpha 1b subunit of rainbow trout (*Oncorhynchus mykiss*) that is most highly correlated with branchial Na^+/K^+ ATPase enzyme activity in salmonids after salinity transfer (Richards et al., 2003; Bystriansky et al., 2006). Thus, mRNA levels for this specific subunit is expected to be the most likely indicator of enzyme activity in goldfish experiencing gill remodeling.

Primers for 18S ribosomal RNA were designed from a 551 bp nucleotide sequence obtained from a BLAST search of GenBank (accession no. AF047349): forward primer 5′-GAGCC-TGAGAAACGGCTACC-3′, reverse primer 5′-CCATGGG-TTTAGATATGCTC-3′. The specificity of the primers was verified by cloning and sequencing of the amplified product.

To ensure that residual genomic DNA was not being amplified, control experiments were performed in which reverse transcriptase was omitted during cDNA synthesis. Relative expression of mRNA levels was determined (using 18S RNA as an endogenous standard) by a modification of the Δ-ΔCt method (Pfaffl, 2001). Amplification efficiencies were determined from standard curves generated by serial dilution of plasmid DNA.

Time-differential double fluorescent staining of ionocytes

To determine whether ionocytes were migrating with the ILCM during temperature change or alternatively appearing as newly differentiated cells, the "time-differential double fluorescent staining" technique of Katoh and Kaneko (Katoh and Kaneko, 2003) was adopted with the following modifications. Only one ^{TM}MitoTracker (^{TM}MitoTracker red CMXRos, Molecular Probes, Eugene, OR, USA) was used; fish were exposed to this fluorescent mitochondrion-specific dye for 4 h (1 µmol l^{-1}) at a water temperature of 25°C. Fish were then exposed to running water and the temperature of the water was gradually reduced to 7°C over the next 2 weeks; control fish were maintained at 25°C for 2 weeks. After 2 weeks, fish were euthanized (see above) and gill tissue was removed, fixed and sectioned for immunocytochemistry as described previously while allowing as little exposure to light as possible. To detect NKA-enriched cells, the α5 monoclonal antibody was used in conjunction with the secondary antibody Alexa Fluor 488 (green) coupled to goat anti-mouse IgG (Fisher). Because we previously demonstrated that all NKA-enriched cells in goldfish will stain positively with ^{TM}MitoTracker (D.M. and S.F.P., unpublished observations), this protocol allows time-dependent differential labeling of the ionocytes. Thus, if a cell is stained both red and green, it existed prior to the onset of temperature change whereas if a cell is stained only green (^{TM}MitoTracker negative, NKA positive), it is assumed that it is a new ionocyte that did not exist at the beginning of the experiment.

Chloride fluxes and plasma analysis

To assess the effects of temperature change and gill remodeling on Cl^- efflux ($J_{OUT}Cl^-$), fish were lightly anesthetized and injected intraperitoneally with 40 µCi kg^{-1} of ^{36}Cl (American Radiolabeled Chemicals, St Louis, MO, USA) and allowed to recover for 12 h. Fish were anesthetized [1 ml of ethyl-*P*-amino-benzoate (Sigma), 2.4×10^{-4} mol l^{-1} in 2 l of water] and their vents were sutured shut and glued (^{TM}Vetbond, 3M, St Paul, MN, USA) to eliminate urinary excretion for a maximum of 7 h (the fish were too small to be fitted with urinary catheters). The fish were placed in their chambers and after 3 h water flow was stopped and 10 ml samples were collected for 4 h at hourly intervals to determine the appearance of ^{36}Cl. After 4 h, the fish were euthanized with benzocaine (ethyl-*P*-amino-benzoate, 2.4×10^{-4} mol l^{-1}) and blood samples (~300 µl) were collected by caudal puncture into heparinized syringes. Plasma was obtained by centrifugation (14,000 ***g*** for 3 min) and immediately frozen in liquid N_2. Plasma Cl^- levels were determined using a spectrophotometric method (Zall et al., 1956) modified for microplate use, and Na^+, K^+ and Ca^{2+} concentrations were measured using an atomic absorption spectrometer (AA240 Varian, Mississauga, Canada). ^{36}Cl activity [converted from counts per minute (c.p.m.) to disintegrations per minute (d.p.m.) after quench correction] was measured by liquid scintillation counting (LS 6500 Multi-Purpose Scintillation Counter; Beckman Coulter, USA) using 4 ml of water mixed with 15 ml of scintillation cocktail (Bio-Safe II, Research Products International, IL, USA) or 100 µl of plasma added to 3.9 ml of distilled water and 15 ml of scintillation cocktail. The average rate of appearance of ^{36}Cl in the water was determined from the slope of the linear regressions relating time and ^{36}Cl activity. $J_{OUT}Cl^-$ (in µmol kg^{-1} h^{-1}) was calculated according to the following formula:

$$J_{OUT}Cl^- = (\Delta\text{water } ^{36}\text{Cl} / \text{plasma } ^{36}\text{Cl specific activity}) / \text{fish mass}, \quad (1)$$

where Δwater ^{36}Cl is given as d.p.m. h^{-1}, plasma ^{36}Cl specific activity as d.p.m. µmol l^{-1} and fish mass in kg.

To determine Cl^- influx ($J_{IN}Cl^-$), 0.5 µCi of ^{36}Cl was added to the aerated water and allowed to mix for 15 min. Water samples (10 ml) were taken hourly for 4 h and assessed for ^{36}Cl activity (see above) to obtain an average rate or ^{36}Cl disappearance. For these experiments conducted on a separate group of fish, the vent was not sutured. $J_{IN}Cl^-$ (in µmol kg^{-1} h^{-1}) was calculated according to the following equation:

$$J_{IN}Cl^- = [\Delta\text{water } ^{36}\text{Cl} / \text{water } ^{36}\text{Cl specific activity} / \text{fish mass}, \quad (2)$$

where Δwater ^{36}Cl is given as d.p.m. h^{-1}, water ^{36}Cl specific activity as d.p.m. µmol l^{-1} and fish mass in kg.

Gill paracellular permeability

To assess the effect of temperature change and the associated changes in functional surface area on the paracellular permeability of the gills, fish were anesthetized and injected intraperitoneally with 50 μCi kg^{-1} of the extracellular marker ^{3}H-PEG 4000 (^{3}H-polyethylene glycol 4000; Perkin Elmer, Foster City, CA, USA) using an injection volume of 1.25 ml kg^{-1}. All other aspects of this experimental protocol were identical to the Cl^- efflux experiment previously described. Preliminary experiments (N=6) comparing fish with and without sutured vents demonstrated that PEG efflux was reduced by 94% after suturing the vent. Thus, it is probable that this technique provides a reliable index of branchial PEG efflux.

Data presentation and statistical analysis

Data are presented as means ± 1 standard error of the mean (s.e.m.). SigmaStat (version 3.0, SPSS, Chicago, IL, USA) was used to perform statistical analysis. All data were evaluated by unpaired or one-sample (PCR data) Student's t-tests. In all cases, significance was set at $P<0.05$.

RESULTS

There were obvious differences in gill morphology in the fish acclimated to different temperatures. In fish that were acclimated to warm (25°C) water, the area of ILCM was significantly decreased when compared to the cold (7°C)-acclimated fish (Fig. 1A). The surface area of the ILCM (expressed as a percentage of total interlamellar area) was 94.7±1.4% in fish acclimated to 7°C (N=6) and 28.3±0.9% in fish maintained at 25°C (N=6). Although not quantified in the present study, the reduction of the area of the ILCM resulted in an obvious increase in functional lamellar surface area (SA) in the warm-water fish (compare Fig. 1B and 1C). The reduction in the extent of the ILCM (and the associated increase in the functional SA of the gills) at 25°C was NOT accompanied by a significant increase in the total SA of ionocytes. Indeed, based on mitochondrial staining, the total ionocyte SA was markedly reduced in the fish kept at 25°C (2103±180 compared with 5219±438 μm^2 mm^{-1} of filament; Fig. 2A). The differences in total ionocyte SA at the two temperatures reflected differences in both the density of ionocytes and their individual sizes (Table 1). The ionocytes were situated along the interlamellar regions and lamellar surfaces in the fish acclimated to 25°C but were confined largely to the outer edge of, or within, the ILCM in the fish acclimated to 7°C (Fig. 2B,C). Similar results were obtained when comparing the SA of ionocytes on the basis Na^+/K^+-ATPase (NKA) enrichment. The total SA of the NKA-positive cells (Fig. 3A) was significantly lower in the warm-water fish (1584±170 μm^2 mm^{-1}) than cold-water fish (4146±415 μm^2 mm^{-1}). The decrease in NKA-positive cell SA at 25°C was the result of decreases in their frequency and individual sizes (Table 1). At 7°C, the NKA-positive cells were situated predominantly along the outer edge of the ILCM. The greater SA of the NKA-positive cells in the fish acclimated to 7°C was not matched by an increase in branchial NKA activity; indeed NKA activity was markedly greater in the warm-water fish (Fig. 4A) that exhibited fewer and smaller ionocytes. There was no statistically significant difference in the relative expression of branchial NKA mRNA between the two groups of fish (Fig. 4B); in part a consequence of large variability in the data.

To determine whether the appearance of ionocytes along the edge of the ILCM in the fish acclimated to 7°C was the result of migration of existing cells or differentiation of new cells, a time-differential double fluorescent staining technique was employed. The results demonstrated that the majority of the ionocytes appearing on the ILCM after a reduction in temperature were the result of migration of pre-existing cells [i.e. most of the cells were stained both red (^{TM}Mitotracker) and green (NKA positive)]. Additionally, however, a few new ionocytes appeared within the ILCM, as indicated by the singly green-labeled cells in Fig. 5. In comparison to the control fish kept at 25°C for 2 weeks, there were significantly greater numbers of newly formed ionocytes in fish transferred from 25°C to 7°C (27.5% *versus* 3.5% of total; Fig. 5A).

The effects of acclimation temperature on unidirectional Cl^- fluxes are depicted in Fig. 6; there were no statistically significant differences in $J_{OUT}Cl^-$ (Fig. 6A) or $J_{IN}Cl^-$ (Fig. 6B). The data for $J_{NET}Cl^-$ (calculated on the basis of Cl^- concentration differences

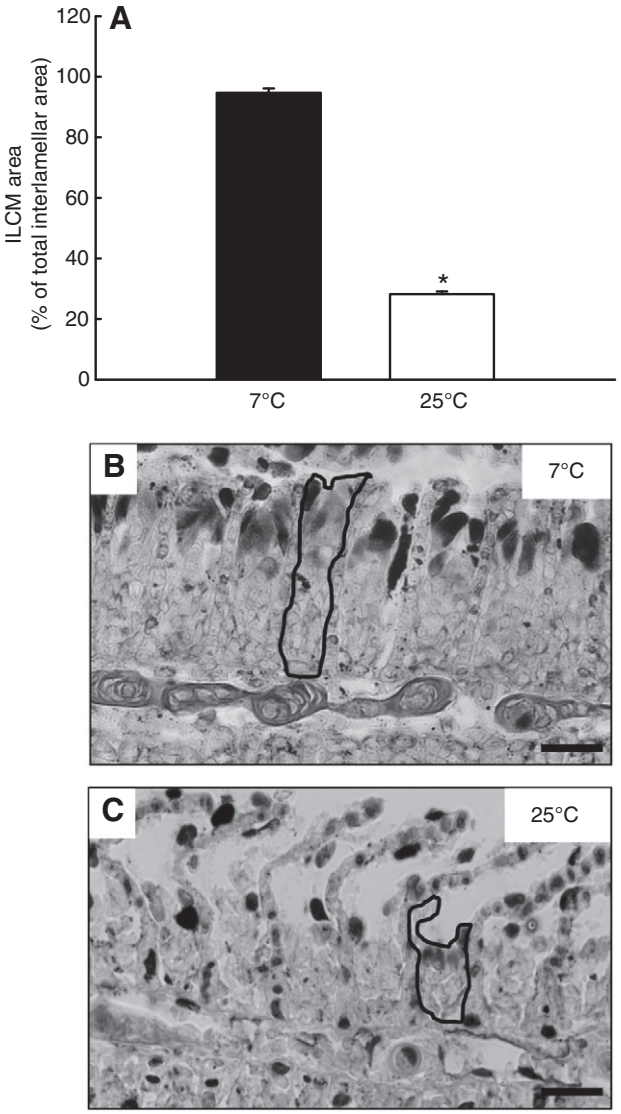

Fig. 1. The effects of acclimation temperature on relative interlamellar cell mass (ILCM) surface area in gills of goldfish (*Carassius auratus*) (A) The surface area of the ILCM (expressed as a percentage of total interlamellar area) was decreased (indicated by asterisk) in fish acclimated to 25°C (N=6) when compared with fish kept at 7°C (N=6); data are presented as means ± 1 s.e.m. (B,C) Representative light micrographs illustrate the marked differences in the extent of the ILCM (single ILCMs outlined in black) in the two groups of fish as well as the obvious increase in functional lamellar surface area in fish acclimated to 25°C; scale bars, 20 μm. The ionocytes are stained black.

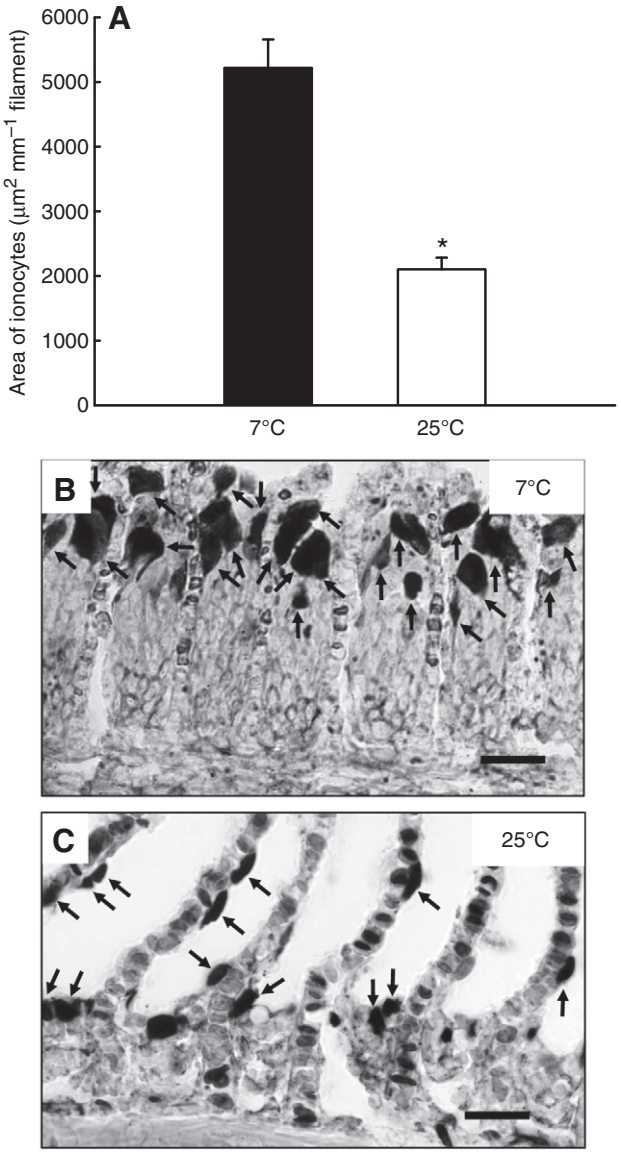

Fig. 2. The effects of acclimation temperature on the surface area of ionocytes (as determined using osmium-zinc iodide staining) and their distribution in goldfish (*Carassius auratus*). (A) The surface area of ionocytes (arrows) was significantly decreased (indicated by asterisk) in fish acclimated to 25°C (N=6) when compared with fish kept at 7°C (N=6); data are presented as means ± 1 s.e.m. (B,C) Representative light micrographs illustrate that the decrease in ionocyte surface area in fish acclimated to 25°C was a result of decreased numbers and sizes of individual cells (see Table 1). Note that the ionocytes were confined to the outer edge of the ILCM in the fish acclimated to 7°C; scale bars, 20 μm.

during flux periods) were highly variable and also indicated no significant differences between the fish acclimated to 7°C (36.4±74.0 μmol kg^{-1} h^{-1}; N=6) and 25°C (–54.4±12.6 μmol kg^{-1} h^{-1}; N=6). Net Cl^- fluxes calculated from the mean data (preventing statistical evaluation) of the unidirectional fluxes were –258 and –433 μmol kg^{-1} h^{-1} at 7°C and 25°C, respectively. The levels of plasma Cl^- in the two groups of fish were consistent with the trends in the Cl^- flux data; plasma [Cl^-] was significantly reduced in the fish acclimated to 25°C (70.5±6.5 mmol l^{-1}) in comparison to the fish at 7°C (85.8±6.9 mmol l^{-1}). Similarly, plasma [K^+] was significantly decreased in the warmer fish whereas plasma [Na^+] and [Ca^{2+}] were increased in fish acclimated to 25°C (Table 2).

Efflux of the extracellular marker PEG, an index of branchial paracellular permeability, was significantly greater (by approximately 2.5-fold) in the fish acclimated to warmer water (Fig. 7).

DISCUSSION

The major findings of this study are that (1) branchial ionocytes remain largely exposed to the water regardless of the presence or absence of an ILCM, (2) the perpetual exposure of ionocytes to the water reflects the migration of pre-existing cells and differentiation of progenitor cells, (3) the ion transporting capacity of the gill (as estimated by ionocyte SA) was not enhanced in fish exhibiting an increase in functional lamellar surface area but instead was markedly reduced, and (4) fish appeared to specifically regulate branchial Cl^- loss in the face of increasing functional lamellar surface area despite a marked increase in general paracellular permeability (PEG efflux).

Modification of the ambient temperature, while promoting adjustments in gill morphology, also will influence a suite of other thermally dependent variables including metabolic rate, cardiac output and ventilation. Such changes are also likely to affect the osmorespiratory compromise. For example, increases in cardiac output and ventilation in warmer water will permit higher metabolic rates but presumably exacerbate the problems of passive branchial salt loss.

The distribution and putative functions of ionocytes in fish with or without an ILCM

In fish acclimated to 7°C, the ionocytes were localized to the outer regions of, and to a lesser extent, within the ILCM whereas in fish lacking an ILCM, the ionocytes were distributed along the lamellar and filament epithelia. Thus, in each situation, the ionocytes are exposed to inspired water where they are presumed to be functional ion transporting cells. The relocation of ionocytes to outer regions of the ILCM in the cold-water acclimated fish is consistent with our hypothesis that ionic uptake would otherwise be severely constrained if lamellar or filament ionocytes were covered by the ILCM. However, the decrease in the surface area of ionocytes in the fish without an ILCM (and hence possessing a greater functional

Table 1. The effects of increased acclimation temperature on the numbers and two-dimensional surface areas of individual ionocytes as identified either using osmium-zinc iodide staining or Na^+/K^+-ATPase immunofluorescence in goldfish (*Carassius auratus*)

		7°C	25°C
Osmium-zinc iodide technique	Average ionocyte surface area (μm^2)	53.2±4.7	37.0±2.8*
	Average number of ionocytes per mm of filament	101.1±3.2	58.0±5.4*
NKA immunofluorescence technique	Average ionocyte surface area (μm^2)	42.1±4.9	25.1±3.3*
	Average number of ionocytes per mm of filament	96.6±5.2	67.1±10.6*

NKA, Na^+/K^+-ATPase.
Data are presented as means ± s.e.m. Significant differences from values at 7°C are indicated by asterisks (P<0.05; N=6 for both groups).

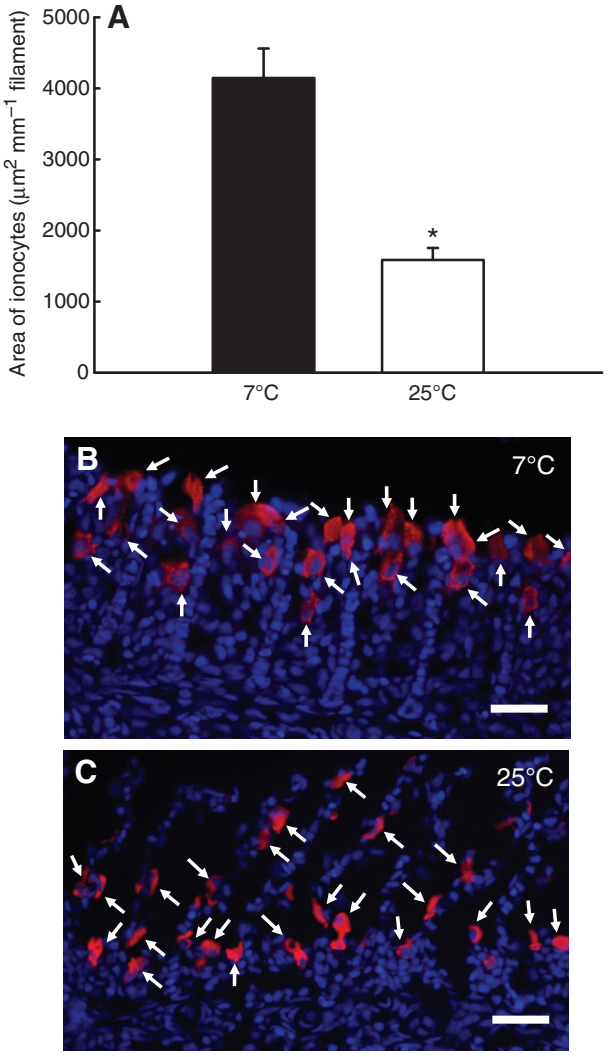

Fig. 3. The effects of acclimation temperature on the surface area of ionocytes (as determined by Na^+/K^+-ATPase immunofluorescence) and their distribution in goldfish (*Carassius auratus*). (A) The surface area of ionocytes was significantly decreased (indicated by asterisk) in fish acclimated to 25°C (N=6) when compared with fish kept at 7°C (N=6); data are presented as means ± 1 s.e.m. (B,C). Representative light micrographs illustrate that the decrease in ionocyte (arrows) surface area in fish acclimated to 25°C was a result of decreased numbers and sizes of individual cells (see Table 1). Note that the ionocytes were confined to the outer edge of the ILCM in the fish acclimated to 7°C; scale bars, 20 μm. Sections were labeled with DAPI-containing mounting media to show cell nuclei (blue).

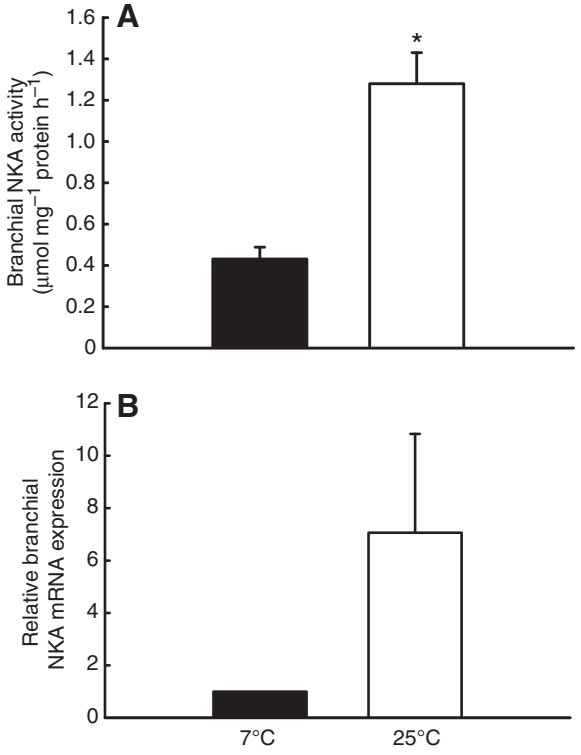

Fig. 4. The effects of acclimation temperature on the (A) branchial Na^+/K^+-ATPase (NKA) activity and (B) relative NKA mRNA levels in goldfish (*Carassius auratus*). (A) Branchial NKA activity was increased (indicated by asterisk) in fish acclimated to 25°C (N=6) when compared with fish acclimated to 7°C (N=6). (B) The expression of NKA mRNA in the fish acclimated to 25°C (N=6) was not significantly increased (P=0.065) when compared to fish at 7°C (N=6) assigned a relative value of 1. Data are presented as means ± 1 s.e.m.

lamellar surface area) did not support the hypothesis that increased ion-transporting capacity is required in such instances to counteract increased passive loss of ions. It is puzzling that the changes in ionocyte SA were not accompanied by similar changes in NKA activities, and clearly this result begs the question as to which metric is a better indicator of branchial ion transport capacity. Given the tight correlation between ionocyte SA and ionic uptake in freshwater teleosts (Perry et al., 1992a; Perry et al., 1992b) and the reports of a lack of correspondence between NKA activities and ionocyte abundance (McCormick, 1995; Sloman et al., 2001), the more reliable indicator would seem to be ionocyte SA. The fact that Cl^- uptake did not significantly increase with increasing ionocyte SA in the present study suggests that one or more other factors (including NKA activity) are regulating this process in the fish experiencing gill remodeling.

Regardless of the underlying explanation for the mismatch between ionocyte SA and NKA activities, the increase in NKA activity with temperature reported here is similar to the previous results of Murphy and Houston (Murphy and Houston, 1974) who demonstrated an approximate 2.5-fold greater branchial NKA activity in goldfish acclimated to 35°C compared with 5°C. It is unclear as to whether a different conclusion would be reached if NKA assays were performed at the respective acclimation temperatures. In common carp, branchial NKA activity was significantly greater in fish acclimated to colder water (15 *vs* 29°C) when assayed at 37°C (maximal activity) but was significantly lower when assayed at the respective acclimation temperatures (Metz et al., 2003).

As in other freshwater teleosts, branchial Cl^- uptake in goldfish is thought to occur *via* an apical membrane electroneutral Cl^-/HCO_3^- exchanger (Maetz and Garcia Romeu, 1964; Garcia Romeu and Maetz, 1964; De Renzis and Maetz, 1973; Preest et al., 2005). The specific genes responsible for Cl^-/HCO_3^- exchange in the fish gill have not been identified with certainty although members of the SLC4 and SLC26 gene families have been implicated by immunocytochemistry (Wilson et al., 2000; Piermarini et al., 2002). In current models of ionic regulation, the apical membrane Cl^-/HCO_3^- exchanger typically is localized to a subset of ionocytes

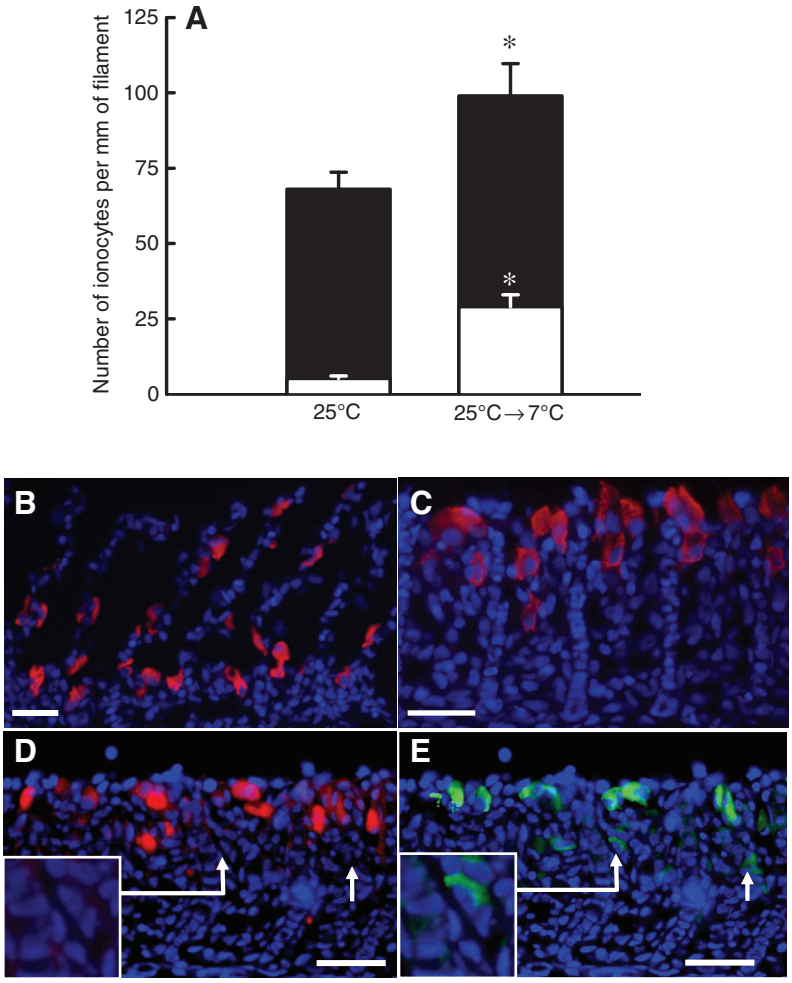

Fig. 5. The effects of decreasing temperature on the redistribution of branchial ionocytes. Live fish were bathed in ™Mitotracker red and over the period of 2 weeks the temperature was brought down from 25°C to 7°C (N=6); the gills were fixed, sectioned and incubated with α5 antibody (green) to label Na^+/K^+-ATPase-positive ionocytes. Thus, after 2 weeks, pre-existing ionocytes would either be single labeled red or doubled labeled red and green, while newly formed ionocytes would be single labeled and appear green only. (A) The lowering of ambient temperature from 25°C to 7°C resulted in a significant increase (indicated by asterisk) in the number of newly formed ionocytes (unfilled portions of bars) while the number of pre-existing ionocytes was also increased (filled portions of bars) when compared to fish maintained at 7°C. Data are presented as means ± 1 s.e.m. (B,C) After 2 weeks, proliferation of the interlamellar cell mass appeared to be accompanied by the migration of pre-existing ionocytes. Scale bar, 20 μm. (D,E) Newly formed ionocytes (arrows) were appearing in the ILCM. Scale bar: 20 μm; All cells were labeled with DAPI mounting medium to show cell nuclei (blue).

that are believed to be functionally analogous to the base secreting (B-type) intercalated cells of the mammalian collecting duct (Perry et al., 2003a; Perry et al., 2003b; Evans et al., 2005; Perry and Gilmour, 2006; Marshall and Grosell, 2006; Tresguerres et al., 2006; Claiborne et al., 2008). Another subset of ionocytes is thought to be analogous to the acid secreting (A-type) intercalated cells of the collecting duct in which an apical membrane Na^+/H^+ exchanger and/or Na^+ channel/VATPase linked process acts to absorb Na^+ (Reid et al., 2003; Lin et al., 2006; Horng et al., 2007; Parks et al., 2007; Yan et al., 2007; Hwang and Lee, 2007). Phenotypically different populations of ionocytes have been identified in several fish species including rainbow trout [*Oncorhynchus mykiss* (Goss et al., 2001)], killifish [*Fundulus heteroclitus* (Laurent et al., 2006)], zebrafish [*Danio rerio* (Hwang and Lee, 2007)] and tilapia [*Oreochromis mossambicus* (Hiroi et al., 2008)]. Different sub-populations of ionocytes have not yet been identified in goldfish but it is conceivable that if existing, the lack of correlation between total ionocyte SA and Cl^- uptake in the fish undergoing gill remodeling may reflect a change in the relative abundance of ionocyte subtypes. For example, unaltered rates of Cl^- uptake in the fish exhibiting increased total ionocyte SA (fish acclimated to 7°C) might simply result from a preferential increase in ionocyte subtypes involved in other ion transport functions (e.g. Na^+ and/or Ca^{2+} uptake). In this regard, it is interesting that whereas plasma Cl^- levels were higher in the fish acclimated to 25°C, plasma Na^+ and Ca^{2+} concentrations were actually lower. Another factor to consider when relating ionocyte SA to rates of Cl^- uptake is their placement within the gill. In fish acclimated to 25°C, the ionocytes are localized on lamellar and filament epithelia in close proximity to blood channels and capillaries, respectively, enabling efficient substrate removal and replenishment. In the fish acclimated to 7°C, the ionocytes are restricted to the edge of the ILCM, which is thought to be devoid of a vascular supply (Sollid et al., 2003). Thus, one should expect that the uptake of Cl^- in the cold-water fish would be constrained by the slow rate of its entry into the circulation. Thus, it is conceivable that the proliferation of ionocytes in the fish acclimated to cold water is a response aimed at aiding ion uptake, given their inhospitable location (at least with respect to blood flow). One can also speculate that the reduced blood supply and associated O_2 deprivation in the vicinity of the ionocytes also contribute to lowering the levels of NKA per cell which might explain the discrepancy between total ionocyte SA and NKA activities. Further studies should attempt to determine if the function of the ionocytes on the ILCM is constrained by inadequate perfusion.

The contribution of cell migration *versus* cell differentiation in the redistribution of ionocytes during gill remodeling

Katoh and Kaneko (Katoh and Kaneko, 2003) described a novel method for establishing the relative contributions of cellular differentiation and transformation to ionocyte replacement in killifish transferred from sea water to fresh water. In the present study, we have adapted their ‘time-differential double fluorescent staining’

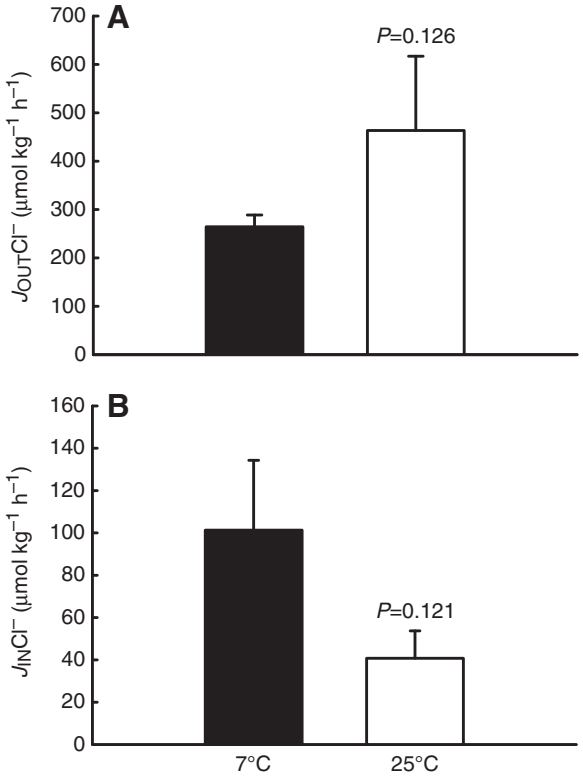

Fig. 6. The effects of acclimation temperature on (A) branchial Cl^- efflux ($J_{OUT}Cl^-$; N=6 for each temperature) and (B) whole body Cl^- influx ($J_{IN}Cl^-$; N=6 for each temperature) in goldfish, *Carassius auratus*. There were no statistically significant differences between the two groups of fish; data are shown as means ± 1 s.e.m.

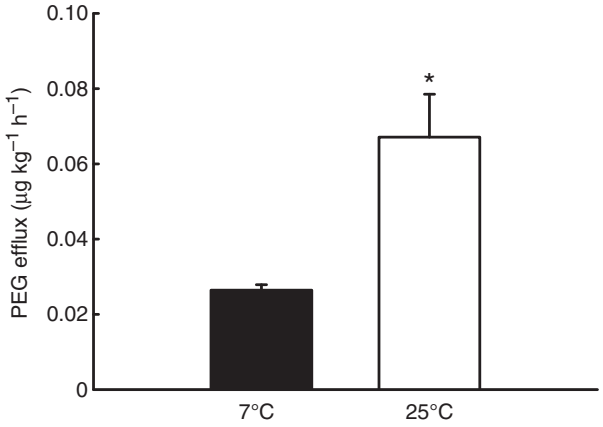

Fig. 7. The effects of acclimation temperature on branchial efflux of polyethylene glycol (PEG) in goldfish, (*Carassius auratus*). Data are presented as means ± 1 s.e.m.; significant difference from 7°C is indicated by an asterisk.

technique to evaluate the dynamics of ionocyte redistribution associated with gill remodeling in goldfish transferred from 25° to 7°C. Our interest was to determine the relative importance of cell migration compared with cell differentiation in the redistribution of ionocytes to the outer edge of the newly formed ILCM. The original method of Katoh and Kaneko (Katoh and Kaneko, 2003) used two fluorescent mitochondrial markers (^{TM}Mitotracker red and ^{TM}Mitotracker green) to distinguish pre-existing from newly formed ionocytes. Although we were able to achieve suitable and persistent (2 weeks) staining by bathing live fish with ^{TM}Mitotracker red, we were less successful when using a second application of ^{TM}Mitotracker green 2 weeks later. Thus, we modified the original protocol of Katoh and Kaneko (Katoh and Kaneko, 2003) by using the α5 antibody (to localize NKA) on tissue sections derived from fish previously subjected to ^{TM}Mitotracker red (two weeks earlier). The interpretation of the data obtained using this double labeling technique relies on the assumption that ^{TM}Mitotracker and the NKA antibody are indeed labeling the same cell type. We believe that this is a reasonable assumption especially given the remarkably similar changes in ionocyte numbers and surface areas determined using the two different techniques (Table 1). Although all cells positive for NKA are likely to be enriched with mitochondria (and hence labeled with ^{TM}Mitotracker), there may be a sub-population of mitochondrion-enriched cells that are not enriched with NKA as observed for the V-ATPase enriched cells of zebrafish (Hwang and Lee, 2007). Even if such cells exist in goldfish, the conclusions regarding cell migration and differentiation would not be altered given the likelihood that all NKA-positive cells are also identified using ^{TM}Mitotracker.

The redistribution of ionocytes from filament to lamellar epithelia was previously described in rainbow trout during acclimation to ion-poor water (Laurent et al., 1995). It was concluded that the appearance of additional ionocytes on the lamellar epithelium in fish acclimated to ion-poor water largely reflected differentiation of filament stem cells and their migration to lamellae. Because the migration of ionocytes from filament to lamella is thought to be relatively slow [e.g. 4 days (Chretien and Pisam, 1986)], it was proposed that the rapid (as early as 12 h) appearance of lamellar ionocytes in the fish kept in ion-poor water may have resulted from differentiation of lamellar stem cells (Laurent et al., 1995) thought to reside in the inner layer of the multi-layered lamellar epithelium (Laurent, 1984). We do not know the origin of the newly formed ionocytes in the fish transferred from 25°C to 7°C in the current study. Interestingly, the new ionocytes, which accounted for about 30% of the total ionocyte population in fish acclimated to 7°C, were never found on the outer edge of the ILCM but instead tended to be located within the cell mass, itself.

Table 2. The effect of increased acclimation temperature on plasma ion levels in goldfish (*Carassius auratus*)

	7°C	25°C
$[Cl^-]$ (mmol l^{-1})	85.8±6.9	70.5±6.5*
$[Na^+]$ (mmol l^{-1})	103.5±3.5	131.2±8.1*
$[K^+]$ (mmol l^{-1})	6.6±0.5	5.1±0.4*
$[Ca^{2+}]$ (mmol l^{-1})	5.8±1.0	11.0±1.1*

Data are presented as means ± 1 s.e.m. Significant differences from values at 7°C are indicated by asterisks (P<0.05; N=11 for all groups).

Paracellular permeability and transepithelial Cl^- fluxes in fish with or without an ILCM

In accordance with the theory, the large difference in functional lamellar surface area in the fish acclimated to 7°C or 25°C resulted in a markedly increased branchial efflux of the paracellular flux marker PEG (Wood et al., 1998) in the warm-water-acclimated fish. Although not quantified in the present study, the extent of gill remodeling in goldfish acclimated to the two temperatures appeared qualitatively to be similar to the degree of gill remodeling observed in crucian carp exposed to hypoxia (Sollid et al., 2003). Thus, it

seems likely that the increase in PEG efflux at higher temperature simply reflected the increased functional surface area. However, the paracellular efflux of Cl^- at higher temperature was statistically constant and did not vary with the presumed increase in surface area. Thus, these results provide evidence for a specific regulation of Cl^- permeability as surface area increases so as to minimize the paracellular loss of Cl^-.

The rate and specificity of solute movement through paracellular pathways is thought to be governed by several families of proteins that constitute tight junctions (Anderson et al., 2004). The two most widely studied tight junction protein families are the claudins and occludin (Gonzalez-Mariscal et al., 2003). Recently, claudins or occludin have been identified in the gills of a variety of fish species where they have been implicated in regulating paracellular salt permeability during salinity transfer (Bagherie-Lachidan et al., 2008; Lundgreen et al., 2008; Tipsmark et al., 2008a; Tipsmark et al., 2008b; Tipsmark et al., 2008c) or ionic imbalance imposed by food deprivation (Chasiotis and Kelly, 2008). There is emerging evidence that specific claudin proteins can differentially regulate the paracellular movement of anions and cations. For example, over-expression of clauidn-7 in cultured porcine kidney cells causes a decrease in paracellular Cl^- conductance while simultaneously increasing paracellular Na^+ conductance (Alexandre et al., 2005). It would be useful in future studies to determine the effects of gill remodeling on the relative expression of goldfish gill tight junction proteins.

Another factor presumably reducing the paracellular efflux of Cl^- in the warm-water-acclimated fish is a lowering of the blood-to-water diffusion gradient because plasma [Cl^-] was approximately 15 mmol l^{-1} lower (Table 2) in the fish at 25°C. Combined, the lowering of the Cl^- diffusion gradient and selective 'tightening' of the paracellular pathways to Cl^-, provide an effective strategy to reduce the costs of absorbing Cl^- in fish with increased functional surface area. Indeed, the rate of Cl^- uptake was not increased in the fish at 25°C suggesting no additional costs of transporting Cl^-. Although there were no statistically significant changes in Cl^- efflux or influx in the warm-water fish when measured after 2 weeks of acclimation, there was an obvious net negative flux of Cl^- (at least when considering the mean data). Thus, it would appear that the measured levels of plasma Cl^- can only be maintained at steady state *via* supplementary dietary uptake of Cl^-.

This research was supported by NSERC of Canada Discovery and Research Tools and Infrastructure grants to S.F.P. We thank Andrew Ochalski for technical guidance for the microscopy experiments and Jason Popesku for providing the initial goldfish Na^+/K^+-ATPase sequence.

REFERENCES

Alexandre, M. D., Lu, Q. and Chen, Y. H. (2005). Overexpression of claudin-7 decreases the paracellular Cl^- conductance and increases the paracellular Na^+ conductance in LLC-PK1 cells. *J. Cell Sci.* **118**, 2683-2693.

Anderson, J. M., Van Itallie, C. M. and Fanning, A. S. (2004). Setting up a selective barrier at the apical junction complex. *Curr. Opin. Cell Biol.* **16**, 140-145.

Bagherie-Lachidan, M., Wright, S. I. and Kelly, S. P. (2008). Claudin-3 tight junction proteins in *Tetraodon nigroviridis*: cloning, tissue-specific expression, and a role in hydromineral balance. *Am. J. Physiol.* **294**, R1638-R1647.

Booth, J. H. (1979). Circulation in trout gills: the relationship between branchial perfusion and the width of the lamellar blood space. *Can. J. Zool.* **57**, 2183-2185.

Brauner, C. J., Matey, V., Wilson, J. M., Bernier, N. J. and Val, A. L. (2004). Transition in organ function during the evolution of air-breathing: insights from *Arapaima gigas*, an obligate air-breathing teleost from the Amazon. *J. Exp. Biol.* **207**, 1433-1438.

Burleson, M. L. (1995). Oxygen availability: sensory systems. In *Biochemistry and Molecular Biology of Fishes* (ed. P. W. Hochachka and T. P. Mommsen), pp. 1-18. Amsterdam: Elsevier.

Burleson, M. L., Smatresk, N. J. and Milsom, W. K. (1992). Afferent inputs associated with cardioventilatory control in fish. In *The Cardiovascular System* (ed. W. S. Hoar, D. J. Randall and A. P. Farrell), pp. 389-423. San Diego, CA: Academic Press.

Burleson, M. L., Mercer, S. E. and Wilk-Blaszczak, M. A. (2006). Isolation and characterization of putative O_2 chemoreceptor cells from the gills of channel catfish (*Ictalurus punctatus*). *Brain Res.* **1092**, 100-107.

Bystriansky, J. S., Richards, J. G., Schulte, P. M. and Ballantyne, J. S. (2006). Reciprocal expression of gill Na^+/K^+-ATPase alpha-subunit isoforms alpha1a and alpha1b during seawater acclimation of three salmonid fishes that vary in their salinity tolerance. *J. Exp. Biol.* **209**, 1848-1858.

Chasiotis, H. and Kelly, S. P. (2008). Occludin immunolocalization and protein expression in goldfish. *J. Exp. Biol.* **211**, 1524-1534.

Chretien, M. and Pisam, M. (1986). Cell renewal and differentiation in the gill epithelium of fresh- or salt-water-adapted euryhaline fosh as revealed by [^{3}H]-thymidine radioautography. *Biol. Cell* **56**, 137-150.

Claiborne, J. B. (1998). Acid-base regulation. In *The Physiology of Fishes* Vol. 2. (ed. D. H. Evans), pp. 171-198. Boca Ratan, FL: CRC Press.

Claiborne, J. B., Choe, K. P., Morrison-Shetlar, A. I., Weakley, J. C., Havird, J., Freiji, A., Evans, D. H. and Edwards, S. L. (2008). Molecular detection and immunological localization of gill Na^+/H^+ exchanger in the dogfish (*Squalus acanthias*). *Am. J. Physiol.* **294**, R1092-R1102.

De Renzis, G. and Maetz, J. (1973). Studies on the mechanism of chloride absorption by the goldfish gill: relation with acid-base regulation. *J. Exp. Biol.* **59**, 339-358.

Evans, D. H., Piermarini, P. M. and Potts, W. T. W. (1999). Ionic transport in the fish gill epithelium. *J. Exp. Zool.* **283**, 641-652.

Evans, D. H., Piermarini, P. M. and Choe, K. P. (2005). The multifunctional fish gill: dominant site of gas exchange, osmoregulation, acid-base regulation, and excretion of nitrogenous waste. *Physiol. Rev.* **85**, 97-177.

Farrell, A. P., Sobin, S. S., Randall, D. J. and Crosby, S. (1980). Intralamellar blood flow patterns in fish gills. *Am. J. Physiol.* **239**, R428-R436.

Garcia Romeu, F. and Maetz, J. (1964). The mechanism of sodium and chloride uptake by the gills of a fresh-water fish, *Carassius auratus*: I. Evidence for an independent uptake of sodium and chloride ions. *J. Gen. Physiol.* **47**, 1195-1207.

Garcia-Romeu, F. and Masoni, A. (1970). Sur la mise en evidence des cellules a chlorure de la branchie des poissons. *Arch. Anat. Microsc. Morphol. Exp.* **59**, 289-294.

Gilmour, K. M. (1997). Gas exchange. In *The Physiology of Fishes* (ed. D. H. Evans), pp. 101-127. Boca Raton, FL: CRC Press.

Gilmour, K. M. and Perry, S. F. (2007). Branchial chemoreceptor regulation of cardiorespiratory function. In *Sensory Systems Neuroscience* (ed. T. J. Hara and B. Zielinski), pp. 97-151. San Diego, CA: Academic Press.

Gonzalez, R. J. and McDonald, D. G. (1992). The relationship between oxygen consumption and ion loss in a freshwater fish. *J. Exp. Biol.* **163**, 317-332.

Gonzalez-Mariscal, L., Betanzos, A., Nava, P. and Jaramillo, B. E. (2003). Tight junction proteins. *Prog. Biophys. Mol. Biol.* **81**, 1-44.

Goss, G. G., Perry, S. F., Wood, C. M. and Laurent, P. (1992). Mechanisms of ion and acid-base regulation at the gills of freshwater fish. *J. Exp. Zool.* **263**, 143-159.

Goss, G. G., Adamia, S. and Galvez, F. (2001). Peanut lectin binds to a subpopulation of mitochondria-rich cells in the rainbow trout gill epithelium. *Am. J. Physiol.* **281**, R1718-R1725.

Hiroi, J., Yasumasu, S., McCormick, S. D., Hwang, P.-P. and Kaneko, T. (2008). Evidence for an apical Na-Cl cotransporter involved in ion uptake in a teleost fish. *J. Exp. Biol.* **211**, 2584-2599.

Horng, J. L., Lin, L. Y., Huang, C. J., Katoh, F., Kaneko, T. and Hwang, P. P. (2007). Knockdown of V-ATPase subunit A (atp6v1a) impairs acid secretion and ion balance in zebrafish (*Danio rerio*). *Am. J. Physiol.* **292**, R2068-R2076.

Hwang, P. P. and Lee, T. H. (2007). New insights into fish ion regulation and mitochondrion-rich cells. *Comp. Biochem. Physiol.* **148A**, 479-497.

Jonz, M. G., Fearon, I. M. and Nurse, C. A. (2004). Neuroepithelial oxygen chemoreceptors of the zebrafish gill. *J. Physiol.* **560**, 737-752.

Katoh, F. and Kaneko, T. (2003). Short-term transformation and long-term replacement of branchial chloride cells in killifish transferred from seawater to freshwater, revealed by morphofunctional observations and a newly established 'time-differential double fluorescent staining' technique. *J. Exp. Biol.* **206**, 4113-4123.

Laurent, P. (1984). Gill internal morphology. In *Fish Physiology Vol XA* (ed. W. S. Hoar and D. J. Randall), pp. 73-183. New York: Academic Press.

Laurent, P. and Dunel, S. (1980). Morphology of gill epithelia in fish. *Am. J. Physiol.* **238**, R147-R159.

Laurent, P. L., Dunel-Erb, S., Chevalier, C. and Lignon, J. (1995). Gill epithelial cell kinetics in a freshwater teleost, *Oncorhynchus mykiss*, during adaptation to ion-poor water and hormonal treatments. *Fish Physiol. Biochem.* **13**, 353-370.

Laurent, P., Chevalier, C. and Wood, C. M. (2006). Appearance of cuboidal cells in relation to salinity in gills of *Fundulus heteroclitus*, a species exhibiting branchial Na^+ but not Cl^- uptake in freshwater. *Cell Tissue Res.* **325**, 481-492.

Lin, L. Y., Horng, J. L., Kunkel, J. G. and Hwang, P. P. (2006). Proton pump-rich cell secretes acid in skin of zebrafish larvae. *Am. J. Physiol.* **290**, C371-C378.

Lundgreen, K., Kiilerich, P., Tipsmark, C. K., Madsen, S. S. and Jensen, F. B. (2008). Physiological response in the European flounder (*Platichthys flesus*) to variable salinity and oxygen conditions. *J. Comp. Physiol. B* **178**, 909-915.

Maetz, J. and Garcia Romeu, F. (1964). The mechanism of sodium and chloride uptake by the gills of a fresh-water fish, *Carassius auratus*: II. Evidence for NH_4+/Na^+ and HCO_3^-/Cl^- exchanges. *J. Gen. Physiol.* **47**, 1209-1227.

Marshall, W. S. and Grosell, M. (2006). Ion transport, osmoregulation and acid-base balance. In *The Physiology of Fishes* (ed. D. H. Evans and J. B. Claiborne), pp. 177-230. Boca Raton, FL: CRC Press.

McCormick, S. D. (1993). Methods for non-lethal gill biopsy and measurements of Na^+,K^+-ATPase activity. *Can. J. Fish. Aquat. Sci.* **50**, 656-658.

McCormick, S. D. (1995). Hormonal control of gill Na^+/K^+-ATPase and chloride cell function. In *Fish Physiology,* Vol 14*: Cellular and Molecular Approaches to Fish Ionic Regulation* (ed. W. S. Hoar, D. J. Randall and A. P. Farrell), pp. 285-315. New York: Academic Press.

Metz, J. R., van den Burg, E. H., Bonga, S. E. and Flik, G. (2003). Regulation of branchial Na^+/K^+-ATPase in common carp *Cyprinus carpio* L. acclimated to different temperatures. *J. Exp. Biol.* **206**, 2273-2280.
Murphy, P. G. and Houston, A. H. (1974). Environmental temperature and the body fluid system of the fresh-water teleost. V. Plasma electrolyte levels and branchial microsomal (Na^+-K^+) ATPase activity in thermally acclimated goldfish (*Carassius auratus*). *Comp. Biochem. Physiol. B* **47**, 563-570.
Nikinmaa, M. (2006). Gas transport. In *The Physiology of Fishes* (ed. D. H. Evans and J. B. Claiborne), pp. 153-174. Boca Raton, FL: CRC Press.
Nilsson, G. E. (2007). Gill remodeling in fish: a new fashion or an ancient secret? *J. Exp. Biol.* **210**, 2403-2409.
Olson, K. R. (1998). Hormone metabolism by the fish gill. *Comp. Biochem. Physiol.* **119A**, 55-65.
Olson, K. R. (2002). Gill circulation: regulation of perfusion distribution and metabolism of regulatory molecules. *J. Exp. Zool.* **293**, 320-335.
Ong, K. J., Stevens, E. D. and Wright, P. A. (2007). Gill morphology of the mangrove killifish (*Kryptolebias marmoratus*) is plastic and changes in response to terrestrial air exposure. *J. Exp. Biol.* **210**, 1109-1115.
Parks, S. K., Tresguerres, M. and Goss, G. G. (2007). Interactions between Na^+ channels and Na^+-HCO_3^- cotransporters in the freshwater fish gill MR cell: a model for transepithelial Na^+ uptake. *Am. J. Physiol.* **292**, C935-C944.
Perry, S. F. (1997). The chloride cell: structure and function in the gill of freshwater fishes. *Annu. Rev. Physiol.* **59**, 325-347.
Perry, S. F. and Gilmour, K. M. (2002). Sensing and transfer of respiratory gases at the fish gill. *J. Exp. Zool.* **293**, 249-263.
Perry, S. F. and Gilmour, K. M. (2006). Acid-base balance and CO_2 excretion in fish: Unanswered questions and emerging models. *Respir. Physiol Neurobiol.* **154**, 199-215.
Perry, S. F. and McDonald, D. G. (1993). Gas exchange. In *The Physiology of Fishes* (ed. D. H. Evans), pp. 251-278. Boca Raton, FL: CRC Press.
Perry, S. F., Goss, G. G. and Fenwick, J. C. (1992a). Interrelationships between gill chloride cell morphology and calcium uptake in freshwater teleosts. *Fish Physiol. Biochem.* **10**, 327-337.
Perry, S. F., Goss, G. G. and Laurent, P. (1992b). The interrelationships between gill chloride cell morphology and ionic uptake in four freshwater teleosts. *Can. J. Zool.* **70**, 1737-1742.
Perry, S. F., Furimsky, M., Bayaa, M., Georgalis, T., Nickerson, J. G. and Moon, T. W. (2003a). Integrated involvement of Na^+/HCO_3^- cotransporters and V-type H^+-ATPases in branchial and renal acid-base regulation in freshwater fishes. *Biochem. Biophys. Acta* **1618**, 175-184.
Perry, S. F., Shahsavarani, A., Georgalis, T., Bayaa, M., Furimsky, M. and Thomas, S. L. Y. (2003b). Channels, pumps and exchangers in the gill and kidney of freshwater fishes: Their role in ionic and acid-base regulation. *J. Exp. Zool.* **300**, 53-62.
Pfaffl, M. W. (2001). A new mathematical model for relative quantification in real-time RT-PCR. *Nucleic. Acids Res.* **29**, 2002-2007.
Piermarini, P. M., Verlander, J. W., Royaux, I. E. and Evans, D. H. (2002). Pendrin immunoreactivity in the gill epithelium of a euryhaline elasmobranch. *Am. J. Physiol.* **283**, R983-R992.
Preest, M. R., Gonzalez, R. J. and Wilson, R. W. (2005). A pharmacological examination of Na^+ and Cl^- transport in two species of freshwater fish. *Physiol. Biochem. Zool.* **78**, 259-272.
Randall, D. J. and Daxboeck, C. (1984). Oxygen and carbon dioxide transfer across fish gills. In *Fish Physiology* (ed. W. S. Hoar and D. J. Randall), pp. 263-314. New York: Academic Press.
Randall, D. J., Baumgarten, D. and Malyusz, M. (1972). The relationship between gas and ion transfer across the gills of fishes. *Comp. Biochem. Physiol. A* **41**, 629-637.
Reid, S. D., Hawkings, G. S., Galvez, F. and Goss, G. G. (2003). Localization and characterization of phenamil-sensitive Na^+ influx in isolated rainbow trout gill epithelial cells. *J. Exp. Biol.* **206**, 551-559.
Richards, J. G., Semple, J. W., Bystriansky, J. S. and Schulte, P. M. (2003). Na^+/K^+-ATPase α-isoform switching in gills of rainbow trout (*Oncorhynchus mykiss*) during salinity transfer. *J. Exp. Biol.* **206**, 4475-4486.
Sloman, K. A., Desforges, P. R. and Gilmour, K. M. (2001). Evidence for a mineralocorticoid-like receptor linked to branchial chloride cell proliferation in freshwater rainbow trout. *J. Exp. Biol.* **204**, 3953-3961.
Sollid, J. and Nilsson, G. E. (2006). Plasticity of respiratory structures-adaptive remodeling of fish gills induced by ambient oxygen and temperature. *Respir. Physiol. Neurobiol.* **154**, 241-251.
Sollid, J., De Angelis, P., Gundersen, K. and Nilsson, G. E. (2003). Hypoxia induces adaptive and reversible gross morphological changes in crucian carp gills. *J. Exp. Biol.* **206**, 3667-3673.
Sollid, J., Weber, R. E. and Nilsson, G. E. (2005). Temperature alters the respiratory surface area of crucian carp *Carassius carassius* and goldfish *Carassius auratus*. *J. Exp. Biol.* **208**, 1109-1116.
Tipsmark, C. K., Baltzegar, D. A., Ozden, O., Grubb, B. J. and Borski, R. J. (2008a). Salinity regulates claudin mRNA and protein expression in the teleost gill. *Am. J. Physiol.* **294**, R1004-R1014.
Tipsmark, C. K., Kiilerich, P., Nilsen, T. O., Ebbesson, L. O., Stefansson, S. O. and Madsen, S. S. (2008b). Branchial expression patterns of claudin isoforms in Atlantic salmon during seawater acclimation and smoltification. *Am. J. Physiol.* **294**, R1563-R1574.
Tipsmark, C. K., Luckenbach, J. A., Madsen, S. S., Kiilerich, P. and Borski, R. J. (2008c). Osmoregulation and expression of ion transport proteins and putative claudins in the gill of southern flounder (*Paralichthys lethostigma*). *Comp. Biochem. Physiol. A* **150**, 265-273.
Tresguerres, M., Katoh, F., Orr, E., Parks, S. K. and Goss, G. G. (2006). Chloride uptake and base secretion in freshwater fish: a transepithelial ion-transport metabolon? *Physiol. Biochem. Zool.* **79**, 981-996.
Wilson, J. M. and Laurent, P. (2002). Fish gill morphology: inside out. *J. Exp. Zool.* **293**, 192-213.
Wilson, J. M., Laurent, P., Tufts, B. L., Benos, D. J., Donowitz, M., Vogl, A. W. and Randall, D. J. (2000). NaCl uptake by the branchial epithelium in freshwater teleost fish: an immunological approach to ion-transport protein localization. *J. Exp. Biol.* **203**, 2279-2296.
Wood, C. M. (1993). Ammonia and urea metabolism and excretion. In *The Physiology of Fishes* (ed. D. H. Evans), pp. 379-425. Boca Raton, FL: CRC Press.
Wood, C. M., Gilmour, K. M., Perry, S. F., Part, P., Laurent, P. and Walsh, P. J. (1998). Pulsatile urea excretion in gulf toadfish (*Opsanus beta*): Evidence for activation of a specific facilitated diffusion transport system. *J. Exp. Biol.* **201**, 805-817.
Wright, P. A. (1995). Nitrogen excretion: three end products, many physiological roles. *J. Exp. Biol.* **198**, 273-281.
Yan, J. J., Chou, M. Y., Kaneko, T. and Hwang, P. P. (2007). Gene expression of Na^+/H^+ exchanger in zebrafish H^+-ATPase-rich cells during acclimation to low-Na^+ and acidic environments. *Am. J. Physiol.* **293**, C1814-C1823.
Zall, D. M., Fisher, M. D. and Garner, Q. M. (1956). Photometric determination of chloride in water. *Anal. Chem.* **28**, 1665-1678.